

# EFFECTS OF BEAM LOADING AND HIGHER-ORDER MODES IN RF CAVITIES FOR MUON IONIZATION COOLING\*

M. Chung, A. Tollestrup, K. Yonehara, Fermilab, Batavia, IL 60510, USA  
B. Freemire, IIT, Chicago, IL 60616, USA  
F. Marhauser, Muons, Inc., Batavia, IL 60134, USA

## Abstract

Envisioned muon ionization cooling channel is based on vacuum and/or gas-filled RF cavities of frequencies of 325 and 650 MHz. In particular, to meet the luminosity requirement for a muon collider, the muon beam intensity should be on the order of  $10^{12}$  muons per bunch. In this high beam intensity, transient beam loading can significantly reduce the accelerating gradients and deteriorate the beam quality. We estimate this beam loading effect using an equivalent circuit model. For gas-filled cavity case, the beam loading is compared with plasma loading. We also investigate the excitation of higher-order modes and their effects on the performance of the cavity.

## INTRODUCTION

One of the main challenges in building muon collider is to achieve 6-D ionization cooling. A cooling channel should reduce the phase space occupied by the beam by about 6 orders of magnitude from the initial volume at the exit of the front end [1]. Two key 6-D cooling channel designs are currently under detailed study: vacuum cooling channel (VCC) with tapered rectilinear lattices [2], and helical cooling channel (HCC) based on gas-filled RF cavities [3]. In both channels, separate cooling channels are used for  $\mu^+$  and  $\mu^-$ . In the first stage of the 6-D cooling channels, the emittance of a train of muon bunches (21 for the present design study) is reduced until the muon beams can be injected into a bunch merging system. The single muon bunches (one for  $\mu^+$  and one for  $\mu^-$ ) are then sent into the second stage of the 6-D cooling channel (see Fig. 1).

Although the number of muon per bunch is very high for both stages before and after the merge (see Table 1), most ionization cooling studies have not considered intensity-dependent effects. We note that before the merge, multi-bunch effects (beam loading and higher-order mode (HOM) wakefields) are of considerable concern, while after the merge, space-charge effects could be significant.

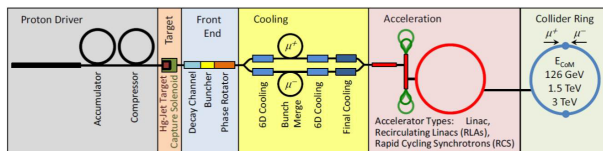


Figure 1: Functional elements of a muon collider complex.

\* Work supported by the Office of Science, U.S. Department of Energy, through the Muon Accelerator Program (MAP).

## BEAM LOADING ESTIMATION

Due to the high bunch currents ( $I_b = 400 \sim 800$  A from Table 1), there are some concerns about beam loading. For muon collider applications, the muon beams are formatted with only 21 bunches in a pulse and the bunch spacing,  $T_b = 1/(325\text{MHz})$  is short compared to the cavity filling time. Therefore, the beam loading does not reach a steady state, and the RF voltage seen by the last bunch will be considerably different from what the first bunch sees.

### Method 1

In the previous study [4], we used an equivalent circuit equation in the slowly varying approximation to estimate the beam loading from the fundamental accelerating mode:

$$\frac{d\tilde{V}_c}{d\tau} + \tilde{V}_c = \tilde{V}_F - \frac{1}{2}Q_L \left[ \frac{R}{Q} \right] \tilde{I}_b, \quad (1)$$

where  $\tilde{V}_c$  is the cavity voltage phasor which is also the sum of the forward ( $\tilde{V}_F$ ) and reverse ( $\tilde{V}_R$ ) voltages. Here,  $\tau = t/T_f$  is time measured in units of filling time  $T_f = 2Q_L/\omega_0$ , and  $Q_L$  is the loaded quality factor of the cavity.

For the case of a point-like bunch with the bunch length much shorter than the bunch spacing, the beam current for a high  $Q_L$  cavity can be given by the single tone signal in phasor notation as follows:

$$I_b(t) \approx \text{Re} \left[ \tilde{I}_b(t) e^{j\omega_0 t} \right] \times H(t), \quad (2)$$

with  $\tilde{I}_b(t) = 2I_{DC} e^{-j\phi_s}$  and  $H(t)$  is the Heaviside step function. Here,  $\phi_s$  is a synchronous phase and  $I_{DC} = Q_b/T_b$  is the average DC current of a bunched beam of charge  $Q_b$ .

Combining Eqs (1) and (2), we can easily obtain the variation of the accelerating voltage  $|\tilde{V}_c| \cos \varphi$  along the beam pulse at  $t > 0$ . Here,  $\varphi$  is the phase angle between  $\tilde{V}_c$  and  $\tilde{I}_b$ , which is  $\varphi = \phi_s$  at  $t = 0$ .

### Method 2

In an alternative way, the beam-induced voltage can also be calculated by applying appropriate initial conditions to the 2nd-order homogenous R-L-C circuit equation for  $t < 0$ :

$$\left\{ \frac{d^2}{dt^2} + \frac{\omega_0}{Q_L} \frac{d}{dt} + \omega_0^2 \right\} V_b = 0. \quad (3)$$

The initial conditions at  $t = 0^+$  are

$$V_b(0^+) = -\frac{Q_b}{C}, \quad (4)$$

Content from this work may be used under the terms of the CC BY 3.0 licence (© 2014). Any distribution of this work must maintain attribution to the author(s), title of the work, publisher, and DOI.

Table 1: Example parameters for 6D cooling channel to provide  $2 \times 10^{12}$  muons per bunch for multi-TeV muon collider. The number of muons is for only single sign.

	325 MHz	650 MHz	Bunch merge	325 MHz	650 MHz	End of channel
Transmission	0.84	0.84	0.8	0.84	0.84	-
Total number of muons	$11.8 \times 10^{12}$	$9.9 \times 10^{12}$	$8.3 \times 10^{12}$	$6.6 \times 10^{12}$	$5.6 \times 10^{12}$	$4.7 \times 10^{12}$
Number of bunches	21	21	21 $\rightarrow$ 1	1	1	1
Bunch length (cm)	7.7	3.2	-	7.7	3.2	3.2

$$\left. \frac{dV_b}{dt} \right|_{t=0^+} = -\frac{dQ_b/dt}{C} = \frac{1}{C} \frac{V_b(0^+)}{R}, \quad (5)$$

where the cavity resistance  $R$  and capacitance  $C$  are related to the unloaded quality factor  $Q_0$  by  $Q_0 = \omega_0 RC$ . For  $Q_L \gg 1$ , the beam-induced voltage is approximated as

$$V_b \approx -2kQ_b \cos(\omega_0 t), \quad (6)$$

where  $k$  is the loss parameter, which can be expressed in several different ways:  $k = \omega_0 R / (2Q_0) = \omega_0 R_{sh} / (4Q_0) = \frac{\omega_0}{4} [R/Q] = 1/(2C)$ . Note that the negative sign in Eq. (6) indicates that the beam tends to decrease the accelerating voltage.

Figures 2 and 3 show that the two methods of calculating the beam loading for the fundamental mode yield nearly the same results. For the 325 MHz RF cavity the stored energy is rather high, so the overall beam loading is about 10 %. On the other hand, the last bunch in the 650 MHz RF cavity sees only 70% of the initial accelerating voltage, which may cause increase in energy spread or change in synchrotron frequency.

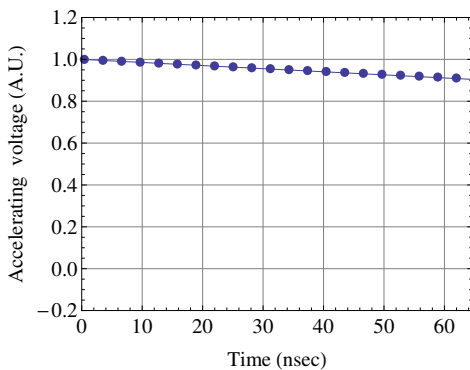


Figure 2: Net accelerating voltages seen by 21 muon beam bunches. Here,  $f_0 = 325$  MHz, cavity length  $l_c = 109.4$  mm,  $[R/Q] = 66.5$  Ohms, and transit time factor  $T = 0.977$ . The total number of muons is  $11.8 \times 10^{12}$  for this case. The line is obtained from method 1, and dots correspond to the calculations based on method 2.

## HIGHER-ORDER MODES

To understand the detailed structure of the higher-order modes, it requires a sophisticated time-domain electromagnetic simulation such as ACE3P/T3P (see, e.g., Fig. 4). When the beam is sub-relativistic regime as in the muon

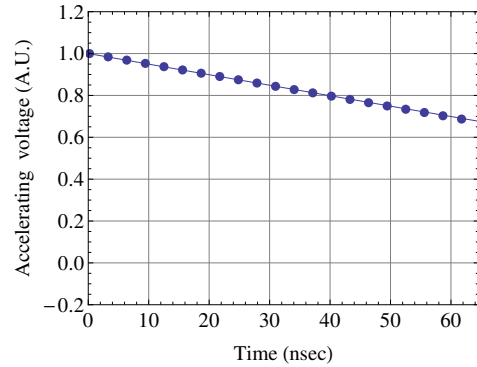


Figure 3: Net accelerating voltages seen by 21 muon beam bunches. Here,  $f_0 = 650$  MHz, cavity length  $l_c = 26.9$  mm,  $[R/Q] = 34.4$  Ohms, and transit time factor  $T = 0.977$ . The total number of muons is  $9.9 \times 10^{12}$  for this case.

cooling channel ( $\beta_b \approx 0.88$ ), it is more challenging as the radiated wakefields might catch up the source particles.

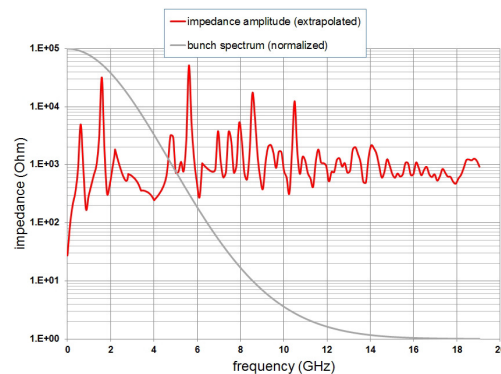


Figure 4: Preliminary calculation of the impedance spectrum excited by a Gaussian bunch with 1 cm rms length and  $\beta_b = 1$  in a 650 MHz cavity.

In the past, several analyses have been made to address wakefields in the muon cooling channel (see, e.g., Ref. [6]). In this proceedings, making use of the analytical wake potentials calculated in Ref. [5], we address the effects of the higher-order modes. The wake potential for a highly relativistic point charge travelling along the  $z$ -axis at radius  $r_b$  is

$$W_z(s; r_b, r_t, \theta_t) = 2 \sum_{mnp} k_{mnp}(r_b, r_t, \theta_t) \cos\left(\frac{\omega_{mnp} s}{c}\right), \quad (7)$$

where  $s > 0$  is the distance between the source charge and a trailing charge. Here,  $k_{mnp}$  is the loss parameter for mode  $TM_{mnp}$ :

$$k_{mnp} = \left( \frac{2 - \delta_{p0}}{1 + \delta_{m0}} \right) \frac{1}{\pi \epsilon_0 l_c j_{m,n}^2 J_m'(j_{m,n})^2} \times J_m \left( \frac{j_{m,n} r_b}{R_w} \right) J_m \left( \frac{j_{m,n} r_t}{R_w} \right) \cos(m\theta_t) \times 2 \left[ 1 - (-1)^p \cos(\omega_{mnp} l_c / c) \right]. \quad (8)$$

For the special case of  $(r_b, r_t, \theta_t) = (0, 0, 0)$  and the fundamental cavity mode  $TM_{010}$ , it can be easily shown that  $k_{010}$  becomes loss parameter  $k$  of the fundamental mode in Eq. (6), i. e.,

$$k_{010} = \frac{1}{4} \frac{(l_c T)^2}{\frac{1}{2} \epsilon_0 \pi R_w^2 l_c J_0'(j_{0,1})^2} = \frac{\omega_0}{4} \left[ \frac{R}{Q} \right], \quad (9)$$

with  $T = \sin(\omega_0 l_c / 2c) / (\omega_0 l_c / 2c)$  and  $\omega_0 = \omega_{010} = j_{0,1} c / R_w$ . Here,  $R_w(l_c)$  is radius (length) of the cavity.

To evaluate the effect of the HOM, we consider the axisymmetric case only ( $m = 0$ ). Figure 5 shows the total beam-induced voltages seen by the last bunch for the cases of  $n = 1, 2, 3$  and  $p = 0$  (left), and  $n = 1, 2, 3$  and  $p = 0, 1$  (right). The fundamental mode term adds coherently and dominates at the end for  $p = 1$  case. The  $n = 2, 3$  modes add but are incommensurate in frequency and so give a varying resultant voltage [8]. The effect of the  $p = 1$  mode is clearly seen in Fig. 5 (right) as a nonharmonic voltage variation.

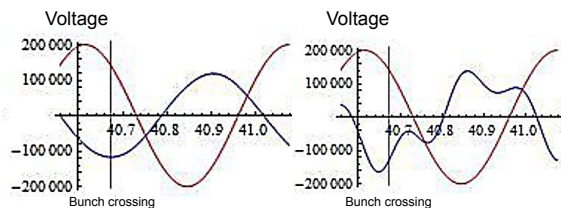


Figure 5: Preliminary calculation of the HOM's in 650 MHz pill-box cavity. The red curves indicate 10% of the applied RF voltages (20 MV/m maximum), and the blue curves indicate the total beam-induced voltages seen by the last bunch. Here, muons per bunch is  $10^{12}$  and  $l_c = 10$  cm.

## PLASMA LOADING

For the HCC, in addition to the beam loading, plasma loading should be taken into account as well. The recent experimental results demonstrate that the effects of the plasma loading are in good agreement with the theoretical prediction, and furthermore they can be minimized by adding small amount of electronegative gas [7]. Based on these experimental observations, a rough calculation of the expected plasma loading in an actual HCC was done [9]. It was shown that the electrons decay quickly due to the attachment process, however ions build up over time. As the energy dissipation by the ions is much smaller due to their heavier masses, overall, no significant plasma loading is observed (see Table 2).

### 05 Beam Dynamics and Electromagnetic Fields

Table 2: Preliminary estimation of the plasma loading effects for muon collider beam parameters. We assume the RF cavities are filled with 180 atm  $H_2$  gas with 1 % dry air.

Parameters	Values			
RF frequency (MHz)	325	325	650	650
muons per bunch	$10^{11}$	$10^{12}$	$10^{11}$	$10^{12}$
$\frac{V_{accel}(last)}{V_{accel}(first)}$ (%)	99.9	99.7	99.7	98.7

## SPACE-CHARGE EFFECTS

Space-charge effects can be important after the bunch merge system. For VCC, it has been shown that the space-charge is not affecting the transverse emittance, but if the longitudinal emittance approaches  $\sim 1.5$  mm, space charge is opposing additional cooling and causes particle loss in longitudinal phase-space [2]. For HCC, the longitudinal dynamics is above transition, so the longitudinal space-charge may act as a focusing force. In addition, we are investigating possible space-charge neutralization process due to the beam-induced plasmas in the gas-filled cavity (see initial result in Fig. 6).

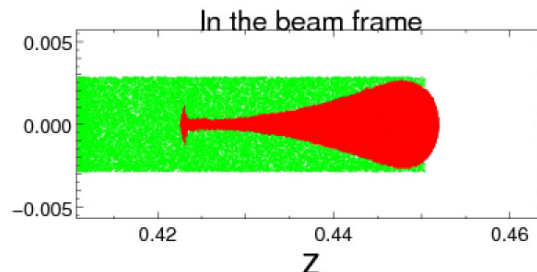


Figure 6: Interaction between muon beam (red) and electrons (green) showing pinching by self-magnetic field in the beam tail. Here, we assume muon beam is in the space-charged dominated regime, and electron dynamics is governed by its mobility. WARP Particle-In-Cell (PIC) code is used.

## REFERENCES

- [1] J-P. Delahaye et al., MAP white paper (2013), FERMILAB-CONF-13-307-APC.
- [2] D. Stratakis et al., in Proc. IPAC 2013 (2013), p. 1553.
- [3] K. Yonehara et al., in Proc. IPAC 2010 (2010), p. 870.
- [4] M. Chung et al., in Proc. IPAC 2013 (2013), p. 1463.
- [5] H. Wang et al., in Proc. PAC 2001 (2001), p. 3024.
- [6] G. R. Werner, arXiv:0906.1007v1 [physics.acc-ph] (2009).
- [7] M. Chung et al., Phys. Rev. Lett. 111, 184802 (2013).
- [8] A. Tollestrup, HPRF 6D Cooling Workshop, <https://indico.fnal.gov/conferenceDisplay.py?confId=7607>
- [9] B. Freemire, Fermilab Joint Experimental-Theoretical Physics Seminar, [http://theory.fnal.gov/jetp/talks/WineAndCheese\\_HPRF.pdf](http://theory.fnal.gov/jetp/talks/WineAndCheese_HPRF.pdf)